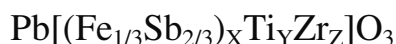
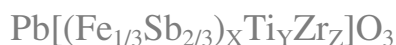


ANDRZEJ OSAK\*, JACEK PIWOWARCZYK\*\*

**STUDIES OF THE DC AND AC HOPPING ELECTRICAL  
 CONDUCTIVITY IN FERROELECTRIC**

**BADANIA STAŁO- I ZMIENNOPRĄDOWEGO  
 HOPPINGOWEGO PRZEWODNICTWA  
 ELEKTRYCZNEGO W FERROELEKTRYCZNYM**

**Abstract**

In the paper results of the dc and ac conductivity measurements in ferroelectric ceramics  $[\text{Pb}(\text{Fe}_{1/3}\text{Sb}_{2/3})_x\text{Ti}_y\text{Zr}_z]\text{O}_3$  with  $x + y + z = 1$ ,  $x = 0.1$  and  $y = 0.43 - 0.47$  are presented. The measurements have been carried out in the temperature range 77–750 K. DC conductivity in the range low temperature obeys Mott's law  $\sigma(0) \sim \exp[-(T_0/T)^{1/4}]$ . The values of  $T_0$  are the order  $10^6$  K. In the high temperature range dc conductivity shows an activated temperature dependence. AC conductivity has been measured in the range of frequency 50 Hz–100 kHz. It is shown that ac conductivity fulfills the relations  $\sigma(\omega) \sim \omega^S$ , where the power exponent depends on temperature and frequency. The values of the density of states at the Fermi level  $N(E_F)$ , the most probable Mott's hopping distance  $R$  and hopping energy  $W$  were also determined.

*Keyword: PZT-PFS ceramics, electrical conductivity, hopping conduction*

**Streszczenie**

W artykule przedstawiono wyniki pomiarów przewodnictwa zmiennoprądowego i stałoprądowego ferroelektrycznej ceramiki  $[\text{Pb}(\text{Fe}_{1/3}\text{Sb}_{2/3})_x\text{Ti}_y\text{Zr}_z]\text{O}_3$  gdzie  $x + y + z = 1$ ,  $x = 0,1$  i  $y = 0,43 - 0,47$ . Pomiarzy zostały wykonane w zakresie temperatur 77–750 K. Przewodnictwo stałoprądowe w niskich temperaturach jest opisane prawem Motta  $\sigma(0) \sim \exp[-(T_0/T)^{1/4}]$ . Wartość  $T_0$  jest rzędu  $10^6$  K. W zakresie wysokich temperatur przewodnictwo stałoprądowe ma charakter aktywacyjny. Przewodnictwo zmiennoprądowe zostało zmierzone w zakresie od 50 Hz do 100 kHz. Przewodnictwo zmiennoprądowe jest opisane zależnością  $\sigma(\omega) \sim \omega^S$ , gdzie wykładnik potęgowy jest zależny zarówno od temperatury, jak i częstotliwości. W pracy wyznaczono również wartości gęstości stanów na poziomie Fermiego  $N(E_F)$ , najbardziej prawdopodobną odległość hoppingu Motta  $R$  i energię hoppingu  $W$ .

*Słowa kluczowe: ceramika PZT-PFS, przewodnictwo elektryczne, przewodnictwo hoppingowe*

\* Dr inż. Andrzej Osak, Wydział Fizyki, Matematyki i Informatyki Stosowanej, Politechnika Krakowska.

\*\* Dr inż. Jacek Piwowarczyk, Katedra Automatyki, Wydział Elektrotechniki, Automatyki, Informatyki i Elektroniki, Akademia Górniczo-Hutnicza.

## 1. Introduction

The synthesis of complex solid solutions gives possibilities for production of ferroelectric ceramics with required electromechanical, optical, dielectric and other properties [1, 2]. The best-known and extensively investigated ceramics is a combination of solid solution of  $\text{PbZrO}_3$  with  $\text{PbTiO}_3$  (PZT). It was also possible, by modification of PZT with relaxor ferroelectric  $\text{Pb}(\text{Fe}_{1/3}\text{Sb}_{2/3})\text{O}_3$ , to produce the ternary system of the composition  $\text{Pb}[(\text{Fe}_{1/3}\text{Sb}_{2/3})_x\text{Ti}_y\text{Zr}_z]\text{O}_3$ ,  $x + y + z = 1$ ,  $x = 0.1$  and  $y = 0.43 - 0.47$  [3]. The results of the previous studies on the dielectric, ferroelectric [4, 5], electromechanical [6, 7] properties and structure [8] of those compounds suggest their possible practical applications. Measurements of the direct current (dc) conductivity and the J-V characteristics for samples with  $y = 0.44$  and  $y = 0.47$  composition are presented in [4, 9]. In paper [10] the preliminary measurements of alternating current conductivity for samples  $y = 0.44$  and  $y = 0.47$  were presented. In this paper studies of the ac conductivity for samples  $y = 0.43 - 0.47$  and dc conductivity at low temperatures are presented and possible carrier transport mechanisms are discussed.

## 2. Direct current (dc) hopping conduction

### 2.1. Impedance and permittivity

The interaction of electric fields with solids may be investigated by using two different types of electrical stimuli.

First, in transient measurements a step function of voltage  $V_0$  is applied at  $t = 0$  to the sample and the resulting time-varying current  $I(t)$  is measured. The ratio  $V_0/I(t)$  measures the impedance resulting from the step function voltage stimuli. It is so called the time domain measurement.

The second approach is to measure impedance directly in the frequency domain by applying single frequency voltage  $V(t) = V_0 \sin \omega t$  to the sample and measuring phase shift  $\varphi$  and amplitude  $I_m$  of the resulting current.

$$I(t) = I_m \sin(\omega t + \varphi) \quad (1)$$

The impedance  $Z(\omega) = V(t)/I(t)$  is a complex quantity equals to

$$Z(\omega) = Z'(\omega) + jZ''(\omega) \quad (2)$$

The impedance is frequently used for presenting data.

The other two quantities usually defined as modulus functions are the complex dielectric constants (dielectric permittivity)

$$\varepsilon(\omega) = \varepsilon'(\omega) - j\varepsilon''(\omega) \quad (3)$$

and the electric modulus  $M(\omega) = \varepsilon^{-1}(\omega)$

$$M(\omega) = M'(\omega) + jM''(\omega) \quad (4)$$

There are two schools of presenting the experimental data.

The dielectric school use the dielectric constant  $\varepsilon(\omega)$ , while the semiconductor school prefers to speak about the conductivity

$$\sigma(\omega) = \sigma'(\omega) - j\sigma''(\omega) \quad (5)$$

These two quantities are related by

$$\varepsilon_0\varepsilon(\omega) = [\sigma(\omega) - \sigma(0)]/j\omega \quad (6)$$

where  $\varepsilon_0$  is the vacuum permittivity and  $\sigma(0)$  is the conductivity  $\sigma(\omega)$  for  $\omega = 0$ . Measurements of the complex  $\varepsilon(\omega)$  function are particularly appropriate for dielectric materials with a very low or vanishing conductivity. The impedance measurements become very popular when the automatic experimental equipment have been developed to measure and analyse the frequency response of ac signal between  $10^{-4}$ – $10^7$  Hz.

## 2.2. Effect of disorder on the electron state and charge transport

The ideal crystal is characterised by regular arrangement of atoms in the lattice and exhibits the translational symmetry. The unperturbed infinite lattice is an idealisation. In reality, the crystal is always perturbed by the lattice defects. The most important point imperfections are: chemical impurities, vacant lattice sites and interstitial atoms. There are also planar imperfections such as dislocations, grain boundaries and crystal surfaces. The feature that the lattice defects have in common is the ability to bind and realise electrons.

The defect levels can combine into the band (impurity band) that can overlap with the band of the localised- or extended states if the defect concentration is sufficiently high. A single lattice defect causes the splitting-off and simultaneous localization of a state from the band edge. With increasing number of lattice defects the number of localised states outside of the band increases and a tail of localized states appears. A distinct energy  $E_c$ , separating localized- and extended states, is called the mobility edge. Defects with large electron binding energies lead to levels which lie deep in the energy gap, whereas defects with low electron binding energy create shallow levels situated near the band energy edge.

In solids, the electrical transport occurs via extended- or localized states or both. The contribution of the extended states to the conductivity is dominant when the Fermi level lies above the mobility edge  $E_c$ . In such conditions the lattice defect acts as a scattering centre for charge carriers and reduce their mean free paths. If the Fermi level lies in the region of localized states, the conductivity is activated with an energy that corresponds to the difference between the Fermi energy and mobility edge

$$\sigma = \sigma_0 \exp\left[-\frac{E_c - E_F}{k_B T}\right] \quad (7)$$

under assumption that the localised states below  $E_c$  make no contribution to the conductivity. In reality, below  $E_c$  there exists phonon-assisted hopping conductivity.

## 2.3. Hopping mechanism

The elementary hopping process may be either a thermally activated jump over the potential barrier (over barrier hopping) or a phonon-assisted tunnelling through the barrier (under barrier hopping). The factor that determines the tunnelling probability is the overlap in the wave functions of the two localised states. The wave function of localised states exponentially decays from the centre as  $\psi \sim \exp(-\alpha r)$ , where  $\alpha$  is the measure of the extent

of localized function (localization length or radius of localization). The transition probability activated hopping process over the potential barrier between states  $E_i$  and  $E_j$  is described by Boltzmann factor  $\exp(-W/k_B T)$ , where  $W = E_i - E_j$ . The transition probability between two centres is a random variable determined by two quantities namely the tunnelling term  $\exp(-2\alpha R)$  and the phonon term  $\exp(-W/k_B T)$  [11]

$$w_{ij} = w_0 \exp\left(-2\alpha R_{ij} - \frac{W}{k_B T}\right) \quad (8)$$

where  $R_{ij}$  is the inter-site distance and  $w_0$  the quantity which depends on interaction of the hopping charge with the lattice.

#### 2.4. Conduction

All models for hopping conduction start from ensemble of centres (sites) that are randomly distributed in space and energy. The application of an electric field causes directional flow of charge carriers by hopping mechanism. The charge transfer depends on temperature as is seen from (8).

At high temperatures, the second exponential in (8) is small compared with the first one so that the current is governed by the random spatial distribution of the localised centres. In this case, the so called  $R$ -hopping occurs and conductivity is determined by the nearest-neighbour hops exhibiting an activated nature. At low temperatures, the hopping transport will take place within a few  $k_B T$  in the vicinity of the Fermi level. According to Mott the dc conduction is governed by hops for which the exponent in (8) becomes minimal. In this case (so called  $R$ - $\epsilon$  hopping) we obtain the famous Mott  $T^{-1/4}$  law [11–13]

$$\sigma = \sigma_0 \exp\left[-\left(\frac{T_0}{T}\right)^{\frac{1}{4}}\right] \quad (9)$$

where  $T_0$  is a constant proportional to the density of states at the Fermi level  $N(E_F)$ ,  $k_B$  is the Boltzmann constant and  $T_0$  equals

$$T_0 = \frac{\lambda^4 \alpha^3}{k_B N(E_F)} \quad (10)$$

The formula (10) has been obtained by other authors and according to the method of calculation, the following values for  $\lambda$  have been found: 2.05 (Mott [12, 13]), 2 (Ambegoaker et al. [14]), 1.84 (Pollak [15]), 2.28 (Seager and Pike [16]), 2.15 (Skal and Shklovski [17]). The derivation of the  $T^{-1/4}$  law requires certain assumptions, i.e. (i) neglecting correlation between the energies of neighbouring sites, (ii) interaction between electrons on defect sites and (iii) neglecting variation of the density of states with energy. The use of Boltzmann's statistics requires that the energy of hops should satisfy the condition  $W \gg 2k_B T$  [18]. Introducing the most probable hopping distance  $R$  and hopping energy  $W$  between sites, Brenig et al. [19] have obtained the following formulæ

$$R = \frac{3}{4} \left(\frac{T_0}{T}\right)^{\frac{1}{4}} \alpha^{-1} \quad (11)$$

and

$$W = \frac{1}{4} \left( \frac{T_0}{T} \right)^{\frac{1}{4}} \beta^{-1} \quad (12)$$

where  $\beta = 1/k_B T$ .

The theoretical study of hopping in a constant electrical field based on the rate equation approach was first developed by Miller and Abraham [20].

$$\frac{\partial P_i(t)}{\partial t} = \sum_i (w_{ij} P_j(t) - w_{ji} P_i(t)) \quad (13)$$

Here  $P_i(t)$  is the probability finding the charge at site  $i$  at time  $t$  and  $w_{ij}$  is the transition rate between sites  $i$  and  $j$ . An exact solution of the master equation for arbitrary selected  $w_{ij}$  is too difficult to find. Therefore it has been studied by either numerical simulations or some approximations [11]. Miller and Abrahams have calculated the transition rate for an electron hop using the deformation potential approximation for the electron-phonon interaction. The electron wave function was taken from the effective-mass theory. According to Miller and Abrahams

$$w_{i,j} = \frac{E^2 A_0^2 w}{\pi \rho s^5 h^5} \exp \left( -2\alpha R_{ij} - \frac{E_i - E_j}{k_B T} \right) \quad (14)$$

Here  $E_1$  is the deformation potential,  $\rho$  is density and  $A_0$  is an exchange integral.

Miller and Abrahams also pointed out that calculation of dc hopping conductivity reduces the problem of calculation of the current in a random-resistor network governed by Kirchhoff laws. The conductances are random variable proportional to the hopping probability and equal to  $g_0 \exp[-s(E_i, E_j)]$ , where  $g_0$  is a constant and  $s$  is a stochastic variable. According to Miller-Abrahams model, a random network is effectively equivalent to set of independent conducting paths, each path carrying electrons from one end of the system to the other via transitions between near-neighbour sites.

The random-resistor network problem of Miller and Abrahams have been usually solved by percolation theory [14, 21, 22], effective medium approximation method [21, 22] and computer simulation (numerical solution of finite network) [14, 16, 23, 24].

Application of the percolation theory was first proposed by Ambegaoker et al. [14], Shklovski and Efros [25] and Seager and Pike [16]. This method has proved to be very effective and now is widely used. At high temperature (the case  $R$ -percolation) the resistances depend on the separation  $R$  between two sites  $\rho \sim \exp(-2\alpha R)$ , whereas at low temperature ( $\epsilon$ - $R$  percolation) the spread of the resistors depend on the spatial as well as the energy difference between the states. Kirkpatrick [21] and Seager and Pike [16] have calculated the conductivity of the cubic lattice of sites (nodes) with random distribution resistors. They studied nearest-neighbour bond percolation. Another effective method for studying hopping conductivity is the effective medium approximation [EMA], which was first applied to the resistor network by Kirkpatrick [21] and Bryksin [11]. In the EMA method one seeks for a uniform system, characterized by a single transition rate which matches the ensemble-averaged behaviour of the random system.

### 3. AC hopping conduction

#### 3.1. Frequency dependence

In general, the ac conductivity decreases with increasing frequency in the case of band conduction, while it increases with increasing frequency in the case of hopping conduction. The available experimental results on the frequency dependence of ac conductivity have revealed a considerable similarity of behaviour for a very wide range of materials, ordered and disordered, conductivity by electrons, holes, ions, involving various types of chemical bonds and various electronic energy level structures [26–34]. The frequency dependence of ac conductivity can be expressed by the empirical formula [18, 30, 33, 34]

$$\sigma(\omega) = A\omega^s \quad (15)$$

where  $s$  is a weak function of temperature approaching unity at low temperature.

The exponent  $s$  is also a function of frequency [36]. In the region, which is normally experimentally accessible, the range of  $s$  is limited to about 0.7–0.9. In the hopping conduction, it is possible to distinguish different characteristic regions of frequency. At extremely low- and low frequencies, the ac conductivity is practically constant; then, there is a region of frequencies, where the conductivity increases strongly with frequencies. Finally, one encounters a region, where the high-frequency cut-off starts and  $s$  decreases to zero with increasing frequency.

#### 3.2. Temperature dependence

The ac conductivity of disordered solids is weak temperature dependent at low temperatures and becoming stronger at higher temperatures. At high temperatures,  $\sigma_{ac}$  tends to the value of dc conductivity and shows an activated temperature dependence

$$\sigma \propto \exp\left(-\frac{\varepsilon}{kT}\right) \quad (16)$$

This dependence follows from the thermal excitation of electrons from the Fermi level into the region of the maximal density of states. In the case of the over barrier hopping, one observes a strong dependence of ac conductivity on temperature; in the multiple-hopping regime, the exponent  $s$  decreases with temperature.

The description of the ac hopping conductivity was first given by Pollak and Geballe [37]. In the pair approximation, the overall conductivity is given by summation over all contribution from isolated pairs each acting parallelly. In this case, one obtains for real part of ac conductivity the expression [32, 33]

$$\sigma = \frac{\pi N^2 e^2}{6\alpha k_B T} \int_0^\infty \frac{R^4 d(\omega\tau)}{1 + \omega^2 \tau^2} \quad (17)$$

where  $N$  is the number of states contributing to ac conductivity,  $\tau$  is the relaxation time equal to  $\tau = \tau_0 \exp(-\alpha R)$ ,  $\tau_0 = \frac{1}{\omega_0}$  and  $\omega_0$  is the phonon frequency. The integral in this expression is sharp-peaked with respect to  $R$  since  $\tau$  depends on  $R$  exponentially.

It means that contribution to  $\sigma(\omega)$  comes from pairs whose spacing is at a particular distance  $R_\omega$

$$R_\omega = \frac{1}{2\alpha} \ln \left( \frac{1}{\omega\tau_0} \right) \quad (18)$$

for which the function  $\frac{\omega\tau}{1+\omega^2\tau^2}$  has the maximum, i.e. for  $\omega\tau = 1$ .

The final expression for ac conductivity is given by

$$\sigma(\omega) = AN^2(E_F)\alpha^{-5}e^2kT\omega \ln^4 \left( \frac{v_{ph}}{\omega} \right) \quad (19)$$

where  $N(E_F)$  is the density of states at the Fermi level.

The quantity  $A$  is a numerical constant for which different values have been obtained by various authors ( $\pi/3$ , Austin and Mott [13];  $\pi^3/96$ , Pollak [38];  $3.66\pi^2/6$ , Butcher and Hayden [39];  $1/24\pi^4$ , Böttger and Bryksin [40]). For the quantum-mechanical tunnelling (QMT) the ratio of imaginary to real part of the conductivity is equal

$$\frac{\sigma_2}{\sigma_1} = \frac{2}{5\pi} \ln \left( \frac{1}{\omega\tau_0} \right) \quad (20)$$

The two site model (pair approximation) is valid at sufficiently high frequencies, where during half a period of oscillation field, the electron can hop solely between nearest neighbours. At low frequencies, during half of period of oscillation, the electron may perform many hops (multiple hopping) and the pair approximation fails.

In contrast to dc current in the case of ac current, a charge carrier has not to be transferred across the sample from electrode to electrode. The main contribution to ac current comes from the electron transition within well conducting clusters of atoms. With increasing frequency, the sizes of cluster increase and the pair approximation gives an incorrect result.

The theories that go beyond the pair approximation, in which multiple hopping processes are included, yield more complete expressions for conductivity [40–45]. For example one has to mention:

1. The method of equivalent resistor random network for analyzing ac conductivity as developed by Pollak [44] and Kirkpatrick [21].
2. Stochastic treatment of hopping conduction first presented by Scher and Lax [46] and Kivelson [47]. In this approach the charge carrier is regarded as a classical particle undergoing a continuous time random walk on the regular lattice.

#### 4. Experimental

The details of preparation of the solid solution  $\text{Pb}[(\text{Fe}_{1/3}\text{Sb}_{2/3})_x\text{Ti}_y\text{Zr}_z]\text{O}_3$ , the system with  $x + y + z = 1$ ,  $x = 0.1$  and  $y = 0.43 - 0.47$  have been reported elsewhere [3]. The SEM photographs of PFS-PZ-yPT ceramics for different Ti concentration have shown the formation of the simple-phase compounds [7]. The average compositions of the samples

determined from the EDS measurements where the same as the nominal compositions. The average grain size was determined as 1–3  $\mu\text{m}$  [7]. Measurements of very weak currents (down to  $10^{-15}\text{A}$ ) were made using a LCHR 6517A Keithley electrometer in the temperature range 77–770 K. The ac conductivity was determined using a BM 507 and BM 595 type Tesla Bridge as well as HP 4363 LCR meters.

## 5. Results

### 5.1. DC conductivity

Direct current conductivity for each samples in the temperature range 77–770 K have been measured. In Fig. 1, the dc conductivity in the range of low temperatures is presented. At low temperatures from the plot  $\ln\sigma$  vs  $(1/T)^{1/4}$  it follows that Mott's law is fulfilled. The value  $\alpha^{-1} = r$ , the Bohr radius of wave functions of localized states estimated according to Hill consideration [43] equals 2.8  $\text{\AA}$ . The most probable hopping distance  $R$  and hopping energy  $W$  between the states calculated from formulae (11) and (12) are presented in Table 1. In Fig. 2 we show the results of dc conductivity measurements for sample  $y = 0.46$  omitted in an earlier paper [4]. From the earlier paper [4] and that presented in Fig. 2 it follows that at the high temperatures, there are two temperature ranges: one with lower- and second with higher activation energies. The values of activation energies for both temperature ranges are listed in Table 2.

Table 1

**The length of the optimal tunnelling distance  $R$ , the average hopping energy  $W$  and values of the density states at the Fermi level  $N(E_F)$  as well as the value of  $T_0$  for  $r = 2.8 \text{ \AA}$**

$y$	$T_0$ [K]	$N(E_F)$ [ $\text{cm}^{-3}\text{eV}^{-1}$ ] dc	$R$ [ $\text{\AA}$ ]		$W$ [eV]	
			123 K	300 K	123 K	300 K
0.43	$2.26 \cdot 10^6$	$2.77 \cdot 10^{21}$	23.8	19.1	0.030	0.059
0.44	$4.50 \cdot 10^6$	$2.70 \cdot 10^{21}$	22.8	18.2	0.036	0.071
0.45	$2.43 \cdot 10^6$	$2.61 \cdot 10^{21}$	24.9	19.9	0.031	0.061
0.46	$2.44 \cdot 10^6$	$2.56 \cdot 10^{21}$	24.9	20.0	0.031	0.061
0.47	$2.20 \cdot 10^6$	$2.54 \cdot 10^{21}$	24.3	19.4	0.030	0.057

Table 2

**Activation energies calculated from dc measurements for high ( $T > 400 \text{ K}$ ) and intermediate temperature ranges ( $220 \text{ K} < T < 400 \text{ K}$ )**

$y$	220 K < $T$ < 400 K	$T > 400 \text{ K}$
	$E$ [eV]	$E$ [eV]
0.43	0.37	0.97
0.44	0.27	1.12
0.45	0.26	1.36
0.46	0.22	1.37
0.47	0.16	1.48

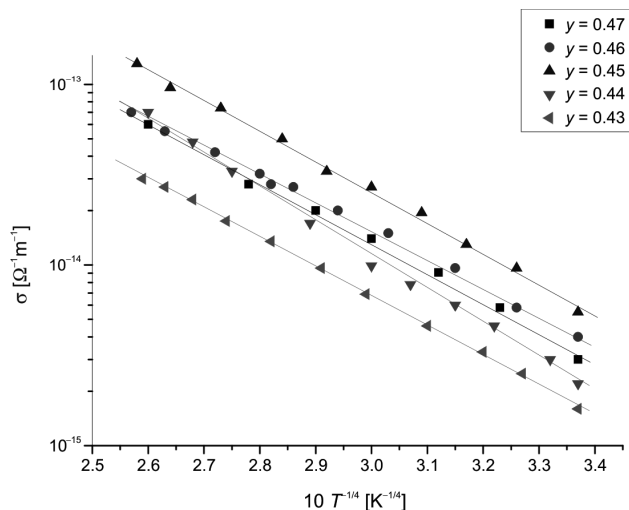


Fig. 1. Low temperature dc conductivity for samples with  $y = 0.43 - 0.47$ .  
Plots of  $\ln \sigma$  versus  $T^{-1/4}$

Rys. 1. Niskotemperaturowe przewodnictwo stałoprądowe dla próbek  $y = 0,43 - 0,47$ .  
Wykres  $\ln \sigma$  od  $T^{-1/4}$

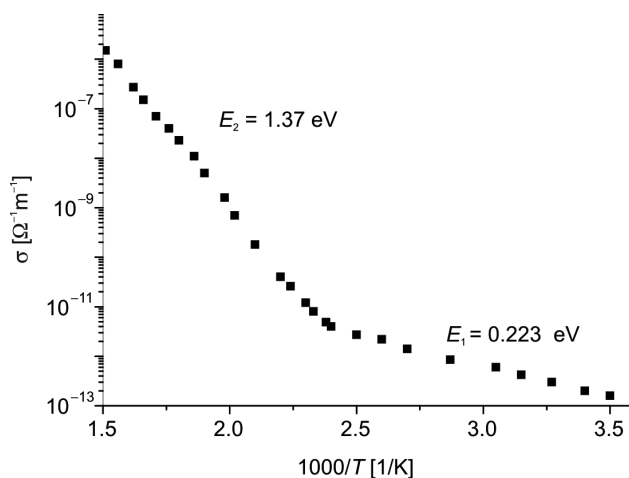


Fig. 2. Temperature dependence of the electric conductivity for sample  $y = 0.46$ .  
Plot of  $\sigma$  versus  $1/T$

Rys. 2. Zależność przewodnictwa elektrycznego od temperatury dla próbki  $y = 0,46$ .  
Wykres  $\sigma$  od  $1/T$

## 5.2. AC conductivity

The temperature dependence of the ac conductivity has been measured in the frequency range 50 Hz–100 kHz and the temperature range 77–770 K. The ac conductivity at high temperatures (285–770 K), for compositions  $y = 0.43 - 0.47$ , are presented in Fig. 3a–e,

respectively, whereas for low temperatures in Fig. 4a–e. In Fig. 3a–e, the magnitude of the dc conductivity from an earlier paper [4] is also included for comparison. The activation energies calculated from the slope of  $\ln \sigma(\omega) \propto 1/T$  are shown in Fig. 3a–e. The results show that with increasing frequencies, for each samples the activation energies  $E$  slightly decreases; e.g. for sample  $y = 0.43$  energy  $E$  decreases from 0.043eV for 0.1 kHz to 0.033eV for 10 kHz (see Fig. 3a). At the highest temperatures (above the Curie temperature), the temperature dependence  $\sigma(\omega)$  becomes strong, while its frequency dependence becomes small almost coinciding with the dc conductivity. At lower temperatures,  $\ln \sigma(\omega)$  is plotted vs.  $\ln T$  (see Fig. 4a–e). In this range,  $\sigma(\omega)$  is proportional to temperature and is not activated in nature. The densities of states  $N(E_F)$  at the Fermi level for temperatures 123 and 300 K, calculated from ac conductivities (formula (19)) are listed in Table 3. The characteristic hopping distance  $R_\omega$  at different frequencies is also listed in Table 3. The frequency dependences of the ac conductivity at selected constant temperatures for sample  $y = 0.43 - 0.47$  are shown in Fig. 5a–e, respectively. The frequency dependent ac conductivity fulfils the power law of the form  $A\omega^s$ . The power law exponents obtained from the least square straight line fits of the data are reported in Table 4. The exponent  $s$  is less than unity and decreases a little with increasing temperature.

The results also show that the transition to frequency independent conduction depends on temperature: the higher temperature, the higher transition frequencies. The value of  $s$  close to one at low temperatures confirms assumption that ac conductivity is predominant due to the relaxation dipole movement. The power law dependence of the ac conductivity on frequency corresponds to the short-range hopping of carriers through trap sites separated by an energy barrier of various heights.

Table 3

**The values of  $N(E_F)$  and the characteristic ac tunnelling distance  $R_\omega$  [Å] at selected frequencies**

$T$	300 K				123 K	
	$10^2$ Hz		$10^4$ Hz		$10^2$ Hz	$10^4$ Hz
$f$	$R_\omega$ [Å]	$N(E_F)$ [cm <sup>-3</sup> eV <sup>-1</sup> ]	$R_\omega$ [Å]	$N(E_F)$ [cm <sup>-3</sup> eV <sup>-1</sup> ]	$N(E_F)$ [cm <sup>-3</sup> eV <sup>-1</sup> ]	$N(E_F)$ [cm <sup>-3</sup> eV <sup>-1</sup> ]
0.43	32.2	$2.67 \cdot 10^{21}$	25.9	$2.67 \cdot 10^{21}$	$2.39 \cdot 10^{21}$	$3.25 \cdot 10^{21}$
0.44	25.3	$3.07 \cdot 10^{21}$	20.2	$4.66 \cdot 10^{21}$	$3.20 \cdot 10^{21}$	$4.00 \cdot 10^{21}$
0.45	32.2	$2.62 \cdot 10^{21}$	25.8	$3.95 \cdot 10^{21}$	$2.54 \cdot 10^{21}$	$3.77 \cdot 10^{21}$
0.46	32.2	$2.29 \cdot 10^{21}$	25.8	$3.39 \cdot 10^{21}$	$2.47 \cdot 10^{21}$	$3.88 \cdot 10^{21}$
0.47	32.2	$1.98 \cdot 10^{21}$	25.7	$2.63 \cdot 10^{21}$	$1.88 \cdot 10^{21}$	$2.75 \cdot 10^{21}$

Table 4

**The value of frequency exponent  $s$  for selected temperatures**

$y = 0.43$		$y = 0.44$		$y = 0.45$		$y = 0.46$		$y = 0.47$	
T [K]	$s$								
77	0.994	77	0.995	77	0.995	77	0.995	77	0.991
293	0.975	293	0.975	298	0.990	293	0.988	298	0.974
673	0.911	673	0.914	663	0.814	473	0.886	623	0.923

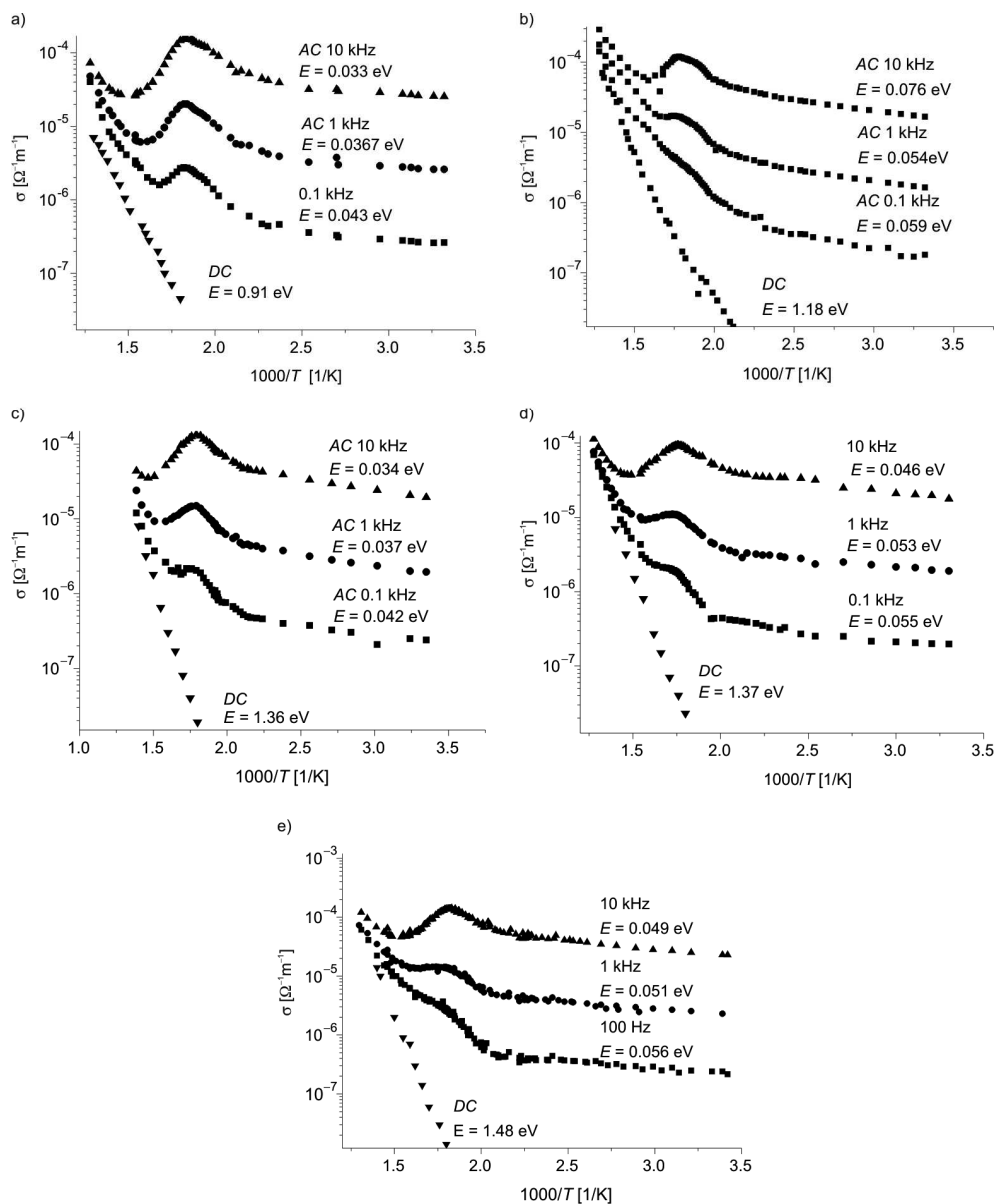


Fig. 3. High temperature dependence of the ac conductivity for sample with composition (a)  $y = 0.43$ , (b)  $y = 0.44$ , (c)  $y = 0.45$ , (d)  $y = 0.46$  and (e)  $y = 0.47$  for frequencies 0.1 kHz, 1 kHz and 10 kHz

Rys. 3. Wysokotemperaturowa zależność przewodnictwa zmiennoprądowego dla próbek o składach (a)  $y = 0,43$ , (b)  $y = 0,44$ , (c)  $y = 0,45$ , (d)  $y = 0,46$ , (e)  $y = 0,47$  oraz częstotliwości 0,1 kHz, 1 kHz i 10 kHz

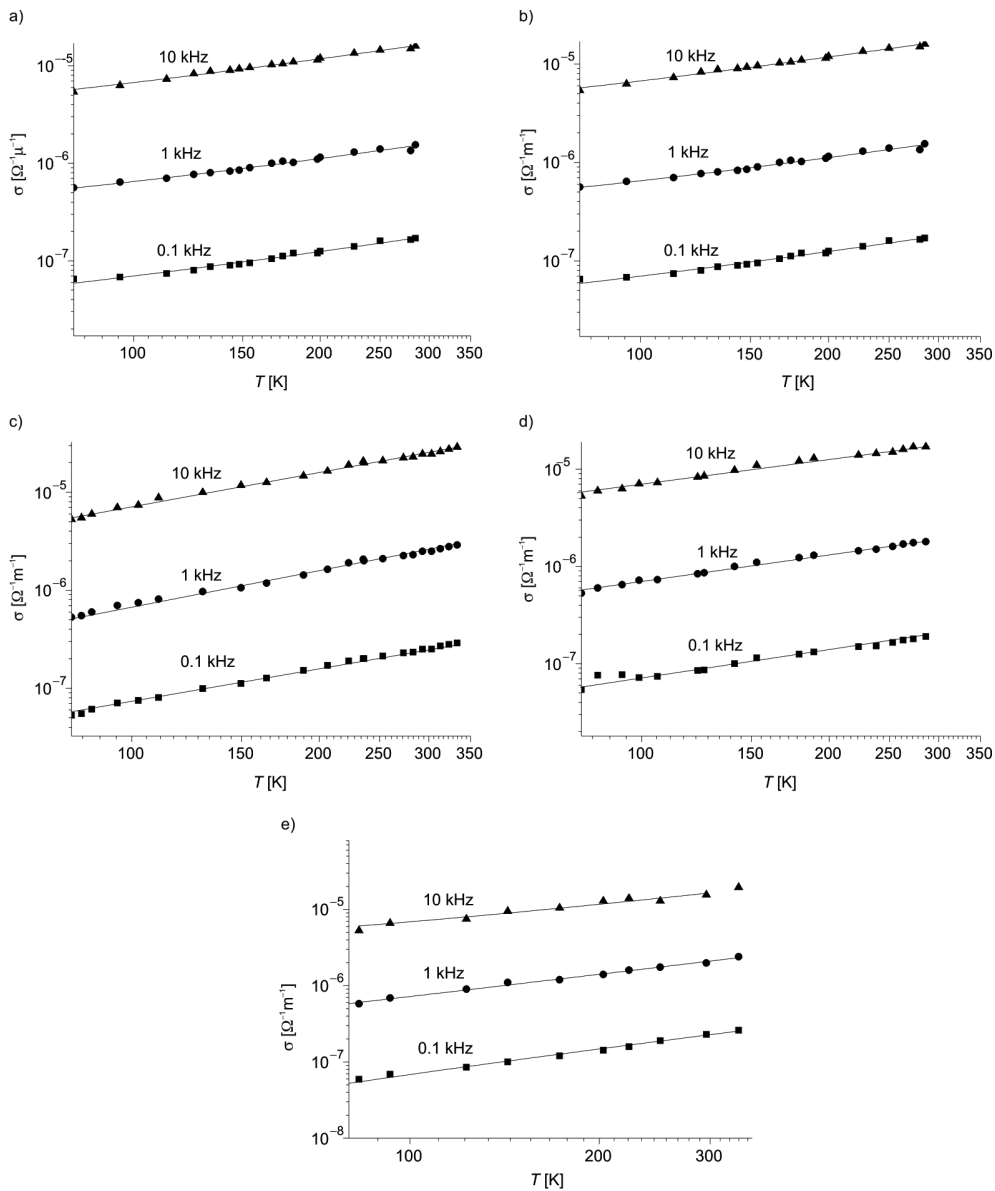


Fig. 4. Low temperature dependence of the ac conductivity for selected frequencies 0.1 kHz, 1 kHz and 10 kHz for Samales with composition (a)  $y = 0.43$ , (b)  $y = 0.44$ , (c)  $y = 0.45$ , (d)  $y = 0.46$  and (e)  $y = 0.47$

Rys. 4. Niskotemperaturowa zależność przewodnictwa zmiennoprądowego dla wybranych częstotliwości 0,1 kHz, 1 kHz i 10 kHz dla próbek o składach (a)  $y = 0,43$ , (b)  $y = 0,44$ , (c)  $y = 0,45$ , (d)  $y = 0,46$  and (e),  $y = 0,47$

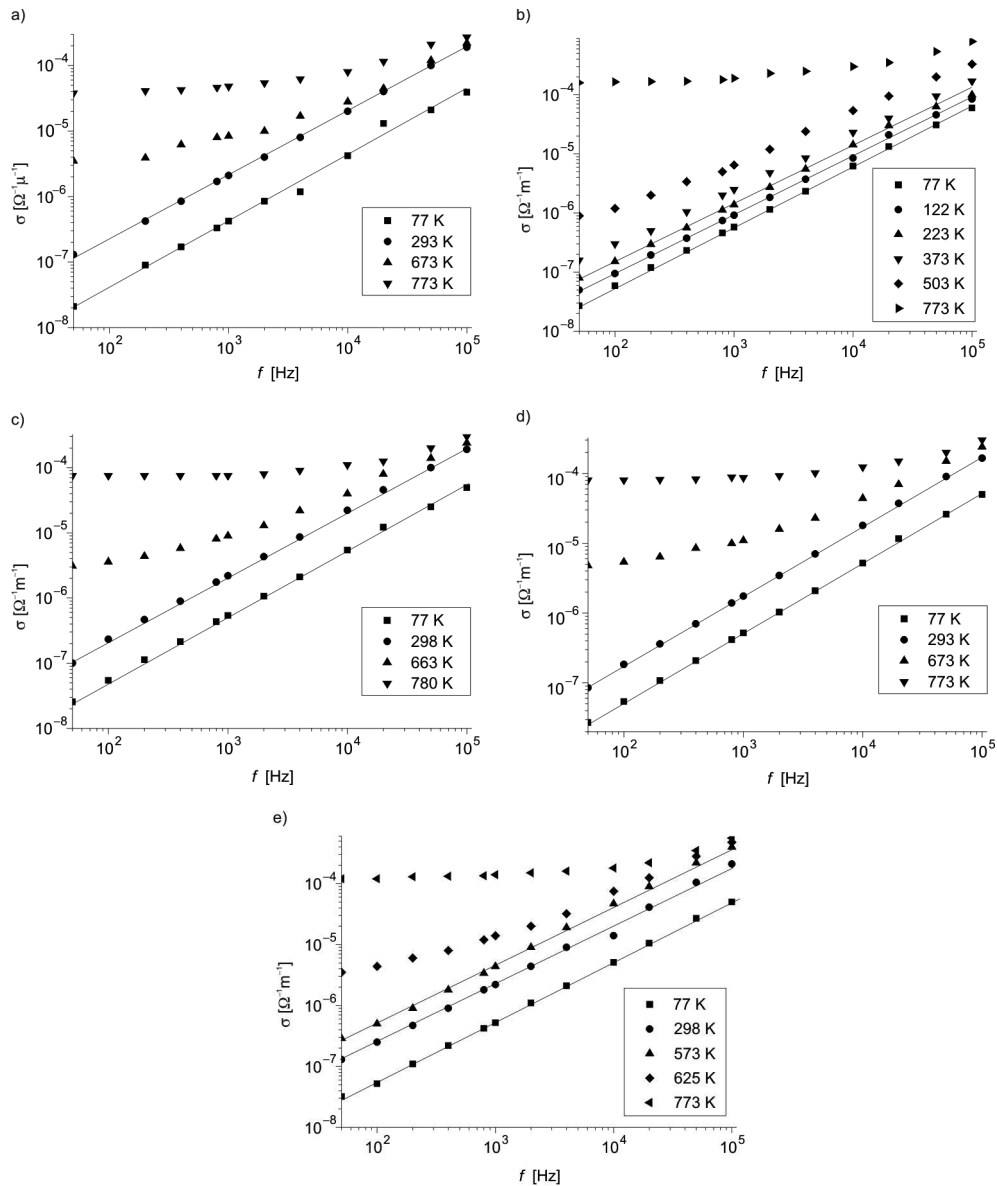


Fig. 5. Frequency dependence of the ac conductivity measured at selected temperatures for sample with composition (a)  $y = 0.43$ , (b)  $y = 0.44$ , (c)  $y = 0.45$ , (d)  $y = 0.46$  and (e)  $y = 0.47$

Rys. 5. Zależność przewodnictwa zmiennoprądowego zmierzonego w wybranych temperaturach od częstotliwości dla próbek o składach (a)  $y = 0.43$ , (b)  $y = 0.44$ , (c)  $y = 0.45$ , (d)  $y = 0.46$  and (e)  $y = 0.47$

## 6. Discussion

1. The investigated samples are ferroelectric complex oxygen compounds. It is expected that ferroelectric properties should affect the measured values of the ac conductivity. In fact, in the vicinity of the phase transition, temperature considerable local maxima of the ac conductivity have been observed for all samples (see Fig. 3a–e). That is because near the Curie temperature, the domain structure break-up and carrier from domain boundary are realised, they became free and take part in the conduction process by trapping mechanism. In the temperature region far from the Curie temperature, the influence of ferroelectric properties is less pronounced. At low temperatures (77–350 K), Mott's law (9) is fulfilled for all samples (see Fig. 1), meaning that variable-range hopping is realised. In this case, an electron prefers to hop to more remote site than to the nearest neighbour one, in order to reduce the energy required from the hop. At high temperatures (above the phase transition), ac conductivity shows an activated character. The activation energy depends on frequency and this energy decreases with increasing frequency.

2. The two-site model is valid at significantly high frequencies, where during half of the period of oscillation of an external field, an electron can hop solely between nearest neighbour sites. In earlier paper [9] we have calculated the density of trapped sites  $N_t$ : 2.97 and  $1.5 \cdot 10^{23}$   $1/m^3$  for samples  $y = 0.44$  and  $y = 0.47$  respectively. If we now

calculate the mean separation distance between sites  $R_S$  from formula  $\left(\frac{4\pi}{3}N_t\right)^{\frac{1}{3}}$  then

we get the following values: 79Å and 113Å for the sample  $y = 0.44$  and  $y = 0.47$  respectively. Comparing the value of  $R_S$  with the spacing  $R_\omega$  (see Table 3) we conclude that  $R_\omega$  does not exceed the value of the  $R_S$ . This result suggests that the two-site hopping model may be used to interpret the experimental data.

3. In the perovskite compound, the most probable defect is  $[O^{2-}]$  oxygen vacancy. The existence of oxygen vacancies lead to the mixed-valence state structure. When  $[O^{2-}]$  oxygen vacancies enter the system, two  $Ti^{5+}$  ions will be found in order to maintain the electrical neutrality. Around the  $[O^{2-}]$  vacancy, the long range potential well is formed. There are likely to be a large number of titanium and zirconium centers within each potential well surrounding the oxygen vacancy. The oxygen vacancy may affect the localization electron at Ti and Zr sites within a radius of several lattice spaces. In such configuration two types of carrier movement is possible:

- a) hopping between Ti or Zr sites within one defect potential well. The average distance passed by a carrier is one lattice space,
- b) hopping between  $Ti^{4+}$  or  $Zr^{4+}$  to  $Ti^{5+}$  or  $Zr^{5+}$  sites. The average distance passed by a carrier is the mean distance between oxygen vacancies. In this way, the dc conductivity may be associated with the hopping between the long range potential well created by oxygen vacancies, while the ac conduction, particularly at low temperatures, can occur through the carrier motion over a shorter range distance between sites in the potential well. Random substitution of ions (Zr, Sb and Fe) in  $Pb[(Fe_{1/3}Sb_{2/3})_xTi_yZr_z]O_3$  lattice causes (i) distribution of transition rate frequency (relaxation times) and associated with the hopping between well created by oxygen vacancies (a mechanism responsible for  $\sigma_1(\omega)$  and dc conductivity) and (ii) a much

larger distribution associated with motion in the potential well (for  $\sigma_2(\omega)$  conduction) [35]. Both relaxation mechanisms give rise to the ac conductivity

$$\sigma(\omega) = \sigma_1(\omega) + \sigma_2(\omega) \quad (22)$$

The decrease of  $s$  with temperature arises owing to higher contribution of  $\sigma_1(\omega)$  at lower frequencies and lower temperatures than at higher frequencies.

4. It is well known [48] that grain inner (bulk grain) and grain boundaries ceramics samples show the different properties. The grain boundary is more defected than the bulk grain; in the grain boundary there are more irregularities in the atomic arrangements. The activation energy of free mobile charge carriers moving through grain boundary is lower than that for charges hopping inside the grains. At different temperatures, there are different mechanism involved in the conduction process. At very low temperature ranges dc conductivity  $T^{-1/4}$  law obeys and only carriers which energies greater than  $2 k_B T$  above Fermi level take part in the electric conduction. The Fermi level position in grain and grain boundary is not so important. In the intermediate temperature range, the sample conduction, is determined by the grain boundary conduction, while at higher temperatures by the inner of the grains. The values of activation energies listed in Table 2 correspond to these two different regions. In the range of high temperatures ac conductivity differs from dc conductivity only slightly. In ceramics materials, dc conductivity mainly depends on the conductivity grain boundaries but at higher temperatures, the diffusive process leads to a more uniformly distribution of defects in grains and grain boundaries and the sample may be treated as homogenous.

## References

- [1] Lines M.E., Glass A.M., *Principles and Applications of Ferroelectrics and Related Materials*, Oxford: Clarendon Press 1977.
- [2] Xu Y., *Ferroelectric materials and their applications*, North Holland, Amsterdam, London, New York 1991.
- [3] Helke G., Röder G., *Ternäre feste Lösungen als leistungsfähige piezokeramische Werkstoffe*, Hermsdorf Techn. Mitt., **54**, 1979, 1729-1734.
- [4] Osak A., Ptak W.S., Osak W., Strzałkowska C., *Dielectric and Electric Properties of Polycrystalline  $[Pb(Fe_{1/3}Sb_{2/3})_xTi_yZr_z]O_3$* , *Ferroelectrics*, **154**, 1994, 247-252.
- [5] Jankowska-Sumara I., *Dielectric and Pyroelectric Properties of  $[Pb(Fe_{1/3}Sb_{2/3})_xTi_yZr_z]O_3$  Ceramics*, *Ferroelectrics*, **345**, 2006, 115-122.
- [6] Jankowska-Sumara I., Osak A., *Field Introduced Electrostrictive Response in  $[Pb(Fe_{1/3}Sb_{2/3})_xTi_yZr_z]O_3$  Ceramics*, *Phase Transitions*, **81**, 2008, 331-340.
- [7] Jankowska-Sumara I., Śmiga W., Bujakiewicz-Korońska R., *The Piezoelectric Effect in  $[Pb(Fe_{1/3}Sb_{2/3})_xTi_yZr_z]O_3$  Ceramics*, *Phase Transition*, **81**, 2008, 1107-1115.
- [8] Osak A.P., Pawelczyk M., Ptak W.S., *Investigation of the Structure, Pyro- and Piezoelectric Properties of a Ferroelectric Ceramic of  $PZT+(FeSb)$* , *Ferroelectrics*, **186**, 1996, 123-126.
- [9] Osak A., Jankowska-Sumara I., *Electrical Transport in Ferroelectric  $Pb[(Fe_{1/3}Sb_{2/3})_xTi_yZr_z]O_3$  Ceramics*, *Phase Transitions*, **82**, 2009, 899-909.
- [10] Osak A., *Hopping Electrical Conductivity in Ferroelectric  $Pb[(Fe_{1/3}Sb_{2/3})_xTi_yZr_z]O_3$* , *Ferroelectrics*, 418, 2011, 52-59.

- [11] Böttger H., Bryksin V.V., *Hopping Conduction in Solids*, Verlag, Berlin 1985.
- [12] Mott N.F., *Conduction in non-crystalline materials*, Phil. Mag., **19**, 1969, 835-852.
- [13] Austin I.G., Mott N.F., *Polarons in Crystalline and Non-crystalline Materials*, Adv. Physics, **18**, 1969, 41-102.
- [14] Ambegaokar V., Halperin B.J., Langer J.S., *Hopping Conductivity in Disordered Systems*, Phys. Rev. B, **4**, 1971, 2612-2620.
- [15] Pollak M., *On the Frequency Dependence of Conductivity in Amorphous Solids*, J. of Non-cryst. Solids, **23**, 1971, 519-542.
- [16] Seager C.H., Pike G.E., *Percolation and Conductivity: A computer study*, Phys. Rev. B, **10**, 1974, 1435-1445.
- [17] Skal A.S., Shklovski B.I., *O Formule Motta Dlja Nizkotemperaturnoj Pryzkowej Prowodimosti. (in Russian)*, Fiz. Tver. Tela, **16**, 1976, 1820-1822.
- [18] Hill R.M., Jonscher A.K., *DC and AC Conductivity in Hopping Electronic Systems*, J. of Non-cryst. Solids, **32**, 1979, 53-69.
- [19] Brenig W., Döhler G.H., Wölfle P., *Thermally Assisted Hopping Transport in Disordered Systems*, Z Physik, **285**, 1973, 381-400.
- [20] Miller A., Abrahams E., *Impurity Conduction at Low Concentrations*, Phys. Rev., **120**, 1960, 745-755.
- [21] Kirkpatrick S., *Percolation and Conduction Rev*, Mod. Physics, **45**, 1973, 574-588.
- [22] Böttger H., Bryksin V.V., *Hopping Conductivity in Ordered and Disordered Solids I*, Phys. Status Solidi (b), **78b**, 1976, 9-56 II b 78, 415-451.
- [23] Butcher P.N., Hayden K.J., Mc Innes J.A., *Analytical Formulae for Dc Hopping Conduction*, Phil. Mag, **36**, 1977, 19-32.
- [24] Maschke K., Overhof H., Thomas P., *On the Variable Range Hopping near the Fermi Energy*, Phys. Status Solidi (b), **62**, 1974, 113-122.
- [25] Sklovski B.J., Efros A.L., Zh. eksp. teor. Fiz, **60**, 1971, 687.
- [26] Rehwald W., Kiess H., Bingelli B., *Frequency Dependent Conductivity in Polymer and Other Disordered Materials*, Z. Phys. B Cond. Matter, **68**, 1987, 143-148.
- [27] Fishchuk J.J., Hertel D., Bässler H., Kadashuk A.K., *Effective-Medium Theory of Hopping Charge Carrier Transport in Weakly Disordered Organic Solids*, Phys. Rev. B, **65**, 2002, 125-201.
- [28] Lin Y.Q., Chen X.M., *Dielectric Relaxation and Polaronic Conduction in Double Perovskite  $\text{La}_2\text{MgMnO}_6$* , Appl. Phys. Letts, **96**, 2010, 142 902-1.
- [29] Ghosh A., Bhattacharya S., Ghosh A., *Tunneling of Large Polarons in Semiconducting Zinc Vanadate Glasses*, J. of Phys. Condensed Matter, 2009, **21**, 145802 (5pp).
- [30] Suchanicz J., *Behavior of  $\text{Na}_{0.5}\text{Bi}_{0.5}\text{TiO}_3$  Ceramics in ac Electric Field*, Ferroelectrics, **209**, 1998, 561-8.
- [31] Pike G.E., *ac Conductivity of Scandium Oxide and New Hopping Model for Conductivity*, Phys. Rev. B, **6**, 1972, 1572-1580.
- [32] Elliott S.R., *A. c. Conduction in Amorphous Chalcogenide and Pnictide Semiconductors*, Adv. Phys., **36**, 1987, 135-218.
- [33] Long A.R., *Frequency-dependent loss in amorphous semiconductors*, Adv. Phys., **31**, 1982, 553-637.
- [34] Elliott S.R., *A Theory of a.c. Conduction in Chalcogenide Glasses*, Phil. Mag., **36**, 1977, 1291-1304.
- [35] Mansingh A., Sayer M., Webb J.B., *Electrical Conduction in Amorphous  $\text{WO}_3$  Films*, J. of Non-Cryst. Solids, **28**, 1978, 123-137.
- [36] Hill R.M., *The Frequency Dependence of Variable Range Hopping Phys*, Stat. Solidi (a), **39**, 1977, 615-620.
- [37] Pollak M., Geballe T.H., *Low-Frequency Conductivity Due to Hopping Processes in Silicon*, Phys. Rev., 1961, **122**, 1742-1753.

- [38] Pollak M., *On the Frequency Dependence of Conductivity in Amorphous Solids*, Phil. Mag., **23**, 1976, 519-542.
- [39] Butcher P.N., Hayden K.J. *Analytical Formulae for d.c. Hopping Conductivity Degenerate Hopping in Wide Bands*, Phil. Mag., **36**, 1977, 657-676.
- [40] Böttger H., Bryksin V.V., Fiz. Tverd. Tela, **17**, 1975, 2920.
- [41] Butcher P.N., *On the Rate Equation Formulation of the Hopping Conductivity Problem*, J. Phys C Solid Stat Phys., **5**, 1972, 1817-1829.
- [42] Dyre J.C., *The Random Free-Energy Barrier Model for ac Conduction in Disordered Solids*, J. of Appl. Phys., **64**, 1988, 2456-2468.
- [43] Hill R.M., *Variable-Range Hopping*, Phys. Stat. Solidi (a), **34**, 1976, 601-613.
- [44] Pollak M., *A Percolation Treatment of the Hopping Conduction*, J. of Non-crystal Solids, **11**, 1972, 1-24.
- [45] Butcher P.N., *Stochastic Interpretation of the Rate Equation Formulation of Hopping Transport Theory*, J. Phys. C Solid State Phys, **7**, 1974, 879-892.
- [46] Scher H., Lax M., *Stochastic Transport in Disordered Solids I Theory II Impurity Conduction*, Phys. Rev. B, **7**, 1973, 4491-502, 4502-19.
- [47] Kivelson S., *Hopping Conductions and Continuous-Time Random Model*, Phys. Rev. B, **21**, 1980, 5755-5767.
- [48] Desu S.B., *Interfacial Effects in Perovskites Key Engineering Materials*, **66-67**, 1992, 375-420.

